



HAL
open science

Rainfall continentality, via the winter Gams angle, provides a new dimension to biogeographical distributions in the western United States

Richard Michalet, Philippe Choler, Ragan Callaway, Thomas Whitham

► To cite this version:

Richard Michalet, Philippe Choler, Ragan Callaway, Thomas Whitham. Rainfall continentality, via the winter Gams angle, provides a new dimension to biogeographical distributions in the western United States. *Global Ecology and Biogeography*, 2021, 30 (2), pp.384-397. 10.1111/geb.13223 . hal-03451970

HAL Id: hal-03451970

<https://hal.science/hal-03451970>

Submitted on 28 Nov 2021

HAL is a multi-disciplinary open access archive for the deposit and dissemination of scientific research documents, whether they are published or not. The documents may come from teaching and research institutions in France or abroad, or from public or private research centers.

L'archive ouverte pluridisciplinaire **HAL**, est destinée au dépôt et à la diffusion de documents scientifiques de niveau recherche, publiés ou non, émanant des établissements d'enseignement et de recherche français ou étrangers, des laboratoires publics ou privés.

1 **Rainfall continentality, via the winter GAMS angle, provides a**
2 **new dimension to biogeographical distributions in the Western**
3 **United States**

4

5 Running Title: Woody plant distributions and continentality

6

7 Richard Michalet^{1*}, Philippe Choler², Ragan M. Callaway³ & Thomas G.⁴
8 Whitham

9

10 ¹University of Bordeaux, UMR CNRS 5805 EPOC, F-33405 Talence, France

11 ²Univ. Grenoble Alpes, Univ. Savoie Mont-Blanc, CNRS, LECA, F-38000
12 Grenoble, France

13

14 ³Division of Biological Sciences, University of Montana, Missoula, MT 59812,
15 USA

16 ⁴Department of Biological Sciences and Merriam-Powell Center for
17 Environmental Research, Northern Arizona University, Flagstaff, Arizona
18 86011 USA

19 *Correspondence: E-mail: richard.michalet@ecologie.u-bordeaux.fr

20

21

22 Abstract

23 **Aim:** Drought stress has focused on water availability during the growing season, thus
24 primarily on summer. However, variation in rainfall continentality can produce striking
25 vegetation differences. We aim to disentangle summer water balance from winter rainfall
26 continentality, to better understand how climate regulated the distributions of woody plants in
27 the western USA.

28 **Location:** Western USA.

29 **Time period:** Actual.

30 **Major taxa studied:** Angiosperms and Conifers.

31 **Method:** We used Redundancy Analysis (RDA) to investigate correlations between rainfall
32 continentality, summer water balance, minimum winter temperature and length of growing
33 season on the distributions of 130 tree and shrub species in 467 plots. Rainfall continentality
34 was calculated using the Gams (1932) index, modified for winter precipitation, and summer
35 water balance with the ratio of summer precipitation to temperature. We estimated Actual
36 EvapoTranspiration (AET), Deficit (DEF), mean annual temperature and rainfall from global
37 gridded datasets and correlated them with RDA axes.

38 **Results:** Rainfall continentality measured with the Gams index and minimum temperatures
39 best explained the contrast between oceanic vegetation in the Pacific Coast Ranges and
40 continental vegetation in the Intermountain Region and Rocky Mountains. Growing Season
41 Length (GSL) was the second strongest factor correlated with vegetation distributions.
42 Summer water balance, despite being the most widely used climatic factor to assess drought
43 stress in biogeography, was the third strongest factor correlating with vegetation classes of the
44 western US. AET was equally correlated with RDA axes 1 and 3, and, thus, could not
45 discriminate between the contrasts in the RDA.

46 **Main conclusions:** Rainfall continentality measured with the winter Gams index provides a
47 more precise metric than summer water balance for understanding the biogeography of woody
48 plants in the western USA. Broadly integrating the Gams index of continentality into plant
49 distributions may improve our understanding of biogeographical distributions and predictions
50 of responses to climate change.

51 **Key-words:** Drought, Growing season length, Minimum temperature, Rainfall
52 continentality, Rain shadow effects, Water balance, Western USA, Winter rainfall

53

54 Introduction

55 For decades, water balance during the growing season has been the key measurement used to
56 quantify drought stress in ecological, biogeographical, physiological and climate change
57 studies, likely due to the primary objective of pioneer biogeographers to separate
58 Mediterranean from temperate climates (Walter & Lieth, 1960; Stephenson, 1990; Rueda,
59 Godoy & Hawkins, 2018; Williams et al., 2020). For example, the ombrothermal diagram
60 proposed by Bagnouls & Gaussen (1953) for the Mediterranean Basin, in Europe and northern
61 Africa, has been widely and successfully used worldwide to describe biogeographical
62 distributions (Walter & Lieth, 1960). Stephenson (1990, 1998) proposed measurements of
63 Actual EvapoTranspiration (AET) and Deficit (DEF), which integrate evaporative demand
64 with available water for plant performance. AET and DEF indices have been applied to water
65 balance in several biological and ecosystem processes and to simulate climate change (Franck
66 & Inouye, 1994; Rehfeldt, Crookston, Warwell, & Evans, 2006).

67 However, indices quantifying water balance during the growing season might be
68 limited in biogeographic explanatory power when growing season length exceeds seven to
69 eight months, because they integrate both the effects of summer water balance and the effects
70 of winter and early spring rainfall. This is particularly important in areas with both
71 Mediterranean and highly continental climates, such as the western USA. In oceanic
72 Mediterranean climates annual AET (AET_y) is highly influenced by the high winter and
73 spring rainfall but not by the very low summer rainfall (AET in winter and in spring
74 contributes to 39 and 36 vs. 2.7% of AET_y, respectively, in southern California, USA; Fig.
75 1a). In contrast, in continental subtropical climates, AET_y is weakly influenced by the low
76 winter and spring rainfall but strongly influenced by the high summer rainfall (AET in winter
77 and in spring contributes to 9.7 and 18 vs. 48.2% of AET_y, respectively, in New Mexico,
78 USA; Fig. 1b). These two regions, located at similar latitude and altitude, have very similar
79 AET_y and DEF_y (Fig. 1c), but they have strikingly different climates in terms of summer
80 water balance and rainfall continentality (Fig. 1d).

81 Rainfall continentality effects, in which continental interior regions are insulated from
82 oceanic influences, is a decrease in precipitation induced by the penetration of low pressure
83 air on a continent (Schermerhorn, 1967; Bach, Price, Dorn, Liu, & Phillips, 2013). Most low
84 atmospheric air pressure systems have oceanic origins, but they can also originate on inland
85 seas, such as the Mediterranean, Black and Caspian seas in Europe (Michalet, 1991; Pache,

86 Michalet, & Aimé, 1996a; Caccianiga et al., 2008). In temperate and Mediterranean climates,
87 rainfall continentality primarily affects winter precipitation, whereas in tropical monsoon
88 climates these effects can also be strong in summer (Michalet, 1991; Bach et al., 2013).
89 Rainfall continentality effects are much stronger where mountain ranges are adjacent to
90 oceans, due to the increase in precipitation with increasing altitude on the windward sides of
91 mountains (orographic effect, Browning & Hill, 1981) and a decrease on their leeward sides
92 (rain shadow effect, Roe, 2005). Since Vapor-Pressure Deficit (VPD) increases and
93 cloudiness decreases along gradients of increasing rainfall continentality, temperature range
94 increases in continental climates, due to increasing irradiance, with colder winter nights and
95 warmer days than in oceanic climates (Waring & Franklin, 1979; Bach et al., 2013). The
96 increase in day temperature, in particular in the spring, increases growing season length,
97 which explains shifts in vegetation belts to higher altitudes in continental mountain ranges
98 than in oceanic ranges (Ozenda, 1985; Grace, 1987; Michalet, 1991; Desplanque, Rolland, &
99 Michalet, 1998; Michalet et al., 2003; He et al., 2016 and see Fig. 2).

100 Precipitation-based continentality creates striking differences in vegetation in a wide
101 range of climates, and this has major ecological and evolutionary consequences. One of the
102 best examples is in the temperate climate of northwestern America, where mountains and
103 distance from ocean creates the difference between the rainforests of the Pacific Coast and the
104 dry coniferous forests of the Rocky Mountains (Daubenmire, 1946; Franklin & Dyness,
105 1973; del Moral & Watson, 1978; Waring & Franklin, 1979). This difference in vegetation is
106 a major component of classification in the US (Brown, Reichenbacher, & Franson, 1998).
107 Similar differences, though less strong, occur at the same latitudes in temperate Europe
108 between the mixed deciduous-evergreen beech-fir (*Fagus sylvatica-Abies alba*) forests of the
109 external (oceanic) Alps and the larch-pine (*Larix decidua-Pinus sylvestris-P. uncinata*) forests
110 of the inner (continental) Alps (Gams, 1932; Ozenda, 1985; Pache et al., 1996a; Michalet,
111 Joud, Gafta, Rolland, & Callaway, 2003).

112 Although precipitation-based, or rainfall continentality and rain shadow effects,
113 produce striking vegetation patterns on several continents, there has been little attention to
114 winter precipitation in biogeographical patterns, likely because plants are generally dormant
115 during the cold season. An important exception is the use of winter vs. summer precipitation
116 to predict shrub vs. grass dominance, respectively, in US deserts and shrub steppe (Neilson
117 1986, 1987; Paruelo & Lauenroth, 1996; Munson et al., 2013; Reinhardt, McAbee, &
118 Germino, 2019). The most direct physiological stress associated to rainfall continentality is

119 likely the much higher VPDs in continental climates that affect stomatal conductance, water
120 uptake and carbon assimilation (Simonin, Santiago, & Dawson, 2009; Muhamed, Le
121 Bagousse-Pinguet, Touzard, & Michalet, 2013; Novick et al., 2016). Also, the frequency of
122 freezing temperatures increases substantially in dry continental air (Bach et al., 2013), and
123 together with higher irradiances, increase photo-inhibition (Manuel et al., 1999). This is
124 highly detrimental for species with high leaf area and Specific Leaf Area (SLA) (Waring,
125 Emmingham, Gholz, & Grier, 1978). Importantly, plants must cope with these constraints
126 during the growing season, since the low cloudiness of continental climates is observed
127 yearlong (Peyre, 1983). *Sequoia sempervirens*, in northern California, is tightly correlated
128 with overcast conditions (Waring & Franklin, 1979; Barbour et al., 2014), perhaps an example
129 of distributional limits imposed by high VPD in continental climates through leaf
130 physiological traits.

131 In Europe there is a history of using variation in annual rainfall as an indicator of
132 rainfall continentality in mountains (Gams, 1932; Ozenda, 1985). In the Alps of Switzerland,
133 Gams (1932) proposed a rainfall continentality index, based on the rate of increase in
134 precipitation with elevation and quantified with the angle of which the co-tangent is equal to
135 the ratio of annual precipitation to elevation. It allows researchers to compare the rainfall
136 continentality of sites differing in elevation, a task that cannot be accomplished with the only
137 comparison of the precipitation of the sites. This is crucial since altitude and rainfall
138 continentality are complex factors that drive different direct factors for plants, both for
139 temperature and humidity. Thus, one main interest of the Gams-angle index is to disentangle
140 in mountain ranges the effects of rainfall continentality from that of decreased precipitation
141 with decreasing altitude (i.e., orographic effect). Gams (1932) showed that the distribution of
142 European beech (*Fagus sylvatica*) was tightly related to variation in the index, with values
143 below 45° in the external Alps where beech dominates the mountain belt, vs. above 45° in the
144 inner Alps where beech is replaced by Scots pine (*Pinus sylvestris*) and European larch (*Larix*
145 *decidua*). Ozenda (1985) generalized the “Gams-angle” approach throughout the Alpine
146 Chain (see also Michalet et al., 2003 and Caccianiga et al., 2008) and Michalet (1991) applied
147 the Gams-angle index to the Mediterranean climate of Morocco.

148 Michalet (1991) also proposed a climagram combining three important dimensions of
149 mountain biogeography (rainfall continentality, altitude and aridity), that depicts the
150 distribution of plant species both in the geographical and ecological spaces, (Fig. 2).
151 Interestingly, plant species have an oblic distribution in the climagram in direct relation with

152 the aridity zones of Emberger (1930), due to their occurrences at lower elevations in oceanic
153 than continental climates. This means that, consistent with Emberger (1930), species have
154 specific water balance requirements, from very humid to sub-humid for oceanic species,
155 humid to semi-arid for semi-oceanic species and sub-humid to arid for continental species
156 (Fig. 2). These specific water balance conditions can occur at low altitude in oceanic climates,
157 due to high precipitation occurring at low altitude, but only at high altitude in continental
158 climates, due to a lower rate of increasing precipitation with increasing altitude. Thus, this
159 climagram allows to better understand the link existing between the humidity (VPD) and cold
160 stress that is only captured by the Gams index of rainfall continentality. Oceanic species are
161 adapted to warmer climates than continental species since the specific water balance
162 requirements can be found at lower elevation for the former than for the latter. Additionally,
163 this climagram allows a display of the above-mentioned shift of vegetation belts to higher
164 altitudes with increasing continentality. This shift likely contributes to the strong vegetation
165 turnover occurring from oceanic to continental climates, since nights are colder in continental
166 than oceanic climates, thus amplifying cold stress for oceanic species. Crucially, Pache et al.
167 (1996a) proposed a seasonal modification of the Gams-angle index that targeted winter
168 precipitation (December to February), which provided a precipitation-based continentality
169 index. We propose that this index provides a better metric than indices of growing season
170 precipitation for assessing biogeographical patterns from areas with high seasonal variation in
171 rainfall due to large ranges in latitude, like those from the Mediterranean Basin in Europe and
172 Africa or from western North-America.

173 Our main objective is to assess the relative importance of rainfall continentality and
174 summer water balance in driving biogeographical distribution in areas subjected to strong
175 variation in winter and summer rainfall. The western USA has striking vegetation contrasts on
176 gradients of rainfall continentality. Rainfall continentality occurs across a seasonal latitudinal
177 gradient in rainfall, temperate in the north, Mediterranean in the southwest and with
178 subtropical influences in the southeast. Thus, this system is very appropriate for assessing our
179 main objective. We sampled vegetation throughout the 11 states of western USA, establishing
180 467 vegetation plots near climate stations from which we extracted several climate indices to
181 correlate them to vegetation composition using Redundancy Analysis (RDA). We partitioned
182 vegetation plots in 16 groups with a cluster conducted on RDA results and mapped their
183 distribution throughout the 11 states. We also extracted data from the Worldclim database for
184 regional spatial variation in the main climate variables, including the Gam index for rainfall

185 continentality in the winter (Pache et al., 1996a). We finally analysed the relationship between
186 the Gams-angle index and AETy, DEFy (Stephenson, 1998), Mean Annual Precipitation
187 (MAP) and Mean Annual Temperature (MAP) that are commonly used in the literature. We
188 made two main hypotheses: (1) variation in rainfall continentality quantified by the Gams-
189 angle index provides a better metric for quantifying vegetation in Western USA than summer
190 water balance (2) variation in rainfall continentality quantified by the Gams-angle index
191 provides a better metric for quantifying vegetation in Western USA than the current accepted
192 metric of water availability during the growing season (AETy and DEFy).

193 Material and methods

194 Study area

195 We focused on 11 states in western USA (Fig. 2). This geographical area, well separated from
196 the American Prairie further east, may be subdivided into three main geographical units: (1)
197 the western Pacific Coast Ranges *sensu lato*, located in the western parts of Washington State
198 (WA), Oregon (OR) and California (CA) and including the coastal ranges *sensu stricto* and
199 the Cascade and Sierra Nevada ranges, (2) the Intermountain Region, including the Great
200 Basin, Colorado Plateau and southern deserts, mostly located in the eastern parts of the former
201 states and south-west Idaho (ID), Nevada (NV), Utah (UT) and Arizona (AZ), (3) the Rocky
202 Mountains to the east of the study area, in eastern ID, Montana (MT), Wyoming (WY),
203 Colorado (CO) and New Mexico (NM). When considering seasonal rainfall distribution and
204 mean temperatures, five main climatic influences characterize the study area following Walter
205 & Lieth (1960), temperate oceanic in the northwest, mostly limited to WA, OR and ID,
206 Mediterranean in the south-west, only in western CA, continental temperate in the northeast,
207 in MT, WY and CO, continental and slightly subtropical in the southeast, in AZ and NM, and
208 arid-desertic in the southern parts of the Intermountain Region, in UT, NV, eastern CA, and
209 southern AZ and NM.

210 Climatic data and vegetation sampling

211 We collected climate data from 800 weather stations in the Western Regional Climate Center
212 (<https://wrcc.dri.edu/>) for the study area. We used the elevation of the stations and, for the
213 period 1971-2000, the precipitation and minimum and maximum temperatures over 12
214 months. To address our main goal, separating rainfall continentality from summer water
215 balance, we calculated for each weather station the Gams-angle rainfall continentality index

216 using winter (December, January and February) precipitation (W GAMS, Pache et al., 1996a),
217 and a summer water balance index, S ARID, calculating the ratio between the precipitation
218 and the mean of maximum temperatures of the three summer months (June, July and
219 August). For cold stress, we used the minimum temperature of the coldest month for cold-
220 tolerance (Tmin), and the number of months with a maximum temperature above 12.5°C for
221 the Growing Season Length (GSL). For rainfall continentality, we calculated W GAMS with
222 winter precipitation using three different formulas depending on elevation (after Michalet et
223 al., 2003), which accounted for non-linearity in increasing precipitation with increasing
224 elevation (Michalet, 1991):

225 - From 900 to 1600 m, we used the original formula of Gams (1932):

226 $Cotg(\alpha) = 4P/A$, Where α is the W GAMS index and P is the winter precipitation in
227 mm and A the elevation in meters.

228 - Below 900 m, we used a modified Gams formula (Michalet, 1991):

229 $Cotg(\alpha) = (4P - ((900-A)/100)*(4P/10))/A$

230 With A = 100 m when elevation below 100 m.

231 - Above 1600 m, we used a second modified Gams formula (Pache, Aimé, & Michalet,
232 1996b):

233 $Cotg(\alpha) = (4P + ((A-1600)/100)*(4P/20))/A$

234 For vegetation sampling, we selected 467 plots near weather stations (see statistical
235 analyses) in order to get the vegetation composition of sites where climate variables were
236 really measured. This sampled the climatic diversity of the total study area, while spatially
237 distributing the sampling. Fieldwork was carried out between 2000 and 2010, at different
238 times of the year depending on the growing season length and leaf phenology of the
239 deciduous species in different areas. We recorded the presence or absence of all tree species
240 and dominant shrubs at less than 5 km from each corresponding weather station, taking care
241 not to sample species at more than 100 m of elevation higher or lower than the weather
242 station. Considering the scale of the study, we sampled at all exposures and on all soil types
243 within the plots.

244 We also extracted from Worldclim2 database (Fick & Hijmans, 2017) the former
245 selected variables for estimating annual Actual EvapoTranspiration (AETy), annual Deficit
246 (DEFy), Mean Annual Temperature (MAT) and Mean Annual Precipitation (MAP) for post-
247 analyses correlations. The water balance-related variables (AETy and DEFy) were calculated
248 according to Stephenson (1990). The Available Water Capacity (AWC) was retrieved from

249 the USDA State Soil Geographic Database (Miller & White, 1998). AWC data for the first
250 100 cm have been used.

251 Statistical analyses

252 We conducted a Principal Component Analysis on the 800 weather stations and four climates
253 indices extracted from the Western Regional Climate Center (W GAMS, S ARID, Tmin and
254 GSL). A cluster analysis was conducted on PCA scores in order to select 467 stations among
255 the climate types. We then performed a Redundancy Analysis (RDA) - also known as a
256 multivariate analysis with respect to instrumental variables - to study species-environment
257 relationships. RDA is a two-table ordination technique in which the environmental table - i.e.,
258 the predicting set of variables - is analyzed by a PCA of a correlation matrix, and the floristic
259 table - i.e., the response set of variables - is analysed by a PCA of a covariance matrix. The
260 algorithm searches for the linear combination of environmental variables that best capture
261 community structure (Dray & Chessel, 2003). The environmental table included the same four
262 climate variables as in the PCA, plus winter precipitation (W PREC). Plant species with a
263 frequency lower than five out of the 467 plots were excluded from the analysis. The final
264 floristic table contained 130 species. To benchmark our results with other studies, we
265 projected AETy, DEFy, MAT and MAP on the three first RDA axes. Multivariate analyses
266 were conducted in R (R core team, 2017) with the library ade4 (Dray & Dufour, 2007).

267 The partitioning of vegetation plots was performed on a dissimilarity matrix estimated
268 with the Jaccard's index (Jaccard, 1901). We used the Partitioning Around Medoids (PAM)
269 technique (Kaufman & Rousseeuw, 2009) implemented in the library CLUSTER (Maechler,
270 Rousseeuw, Struyf, Hubert, & Hornik, 2019) to search for k representative objects or medoids
271 among the observations. The algorithm assigns each observation to the nearest medoid with
272 the objective of minimizing the sum of dissimilarities between groups. The method utilizes a
273 prescribed number of medoids. We found that the value k=16 was providing an ecologically
274 and biogeographically meaningful partition of relevés while retaining a sufficient number of
275 relevés per group.

276 Results

277 In the RDA, the total unconstrained inertia was 5.55 and the sum of eigenvalues was 1.13,
278 indicating that 20.4% of the total floristic variance was explained by environmental variables
279 (Appendix S1). The RDA axes accounted for 40%, 29%, 20%, 8% and 3% of the explained

280 variance. Given the drop between axis 3 and axis 4, we did not consider the last two RDA
281 axes in further analyses. In agreement with our first hypothesis, RDA Axis 1 was more
282 positively correlated with rainfall continentality quantified by the Gams-angle index (W
283 GAMS; $r = 0.99$) than any other variable, negatively with winter precipitation (W PREC; $r = -$
284 0.87) and less so with minimum temperatures (Tmin; $r = -0.63$) (Fig. 4A, Table 1). RDA Axis
285 2 was highly negatively correlated with growing season length (GSL; $r = -0.87$) and less with
286 cold temperature (Tmin; $r = -0.72$).

287 RDA Axes 1-2 were also highly correlated with the plant biogeography of the western
288 USA. The temperate rain forests of the Pacific Coast Ranges and Mediterranean evergreen
289 oak forests (cluster groups 1 and 11, respectively) aggregated on the extreme left of Axis 1. In
290 contrast, the coniferous forest and woodland communities from central Montana and eastern
291 pinion-juniper woodlands in the central and southern Rocky Mountains aggregated on the
292 extreme right of Axis 1 (cluster groups 6 and 10, respectively, Fig. 3a, 4a, b, Tables 1, 2). The
293 upper end of Axis 2 was occupied by the northwestern and eastern subalpine coniferous forest
294 communities (cluster groups 12 and 9, respectively) and the lower end by the subtropical
295 desert communities of the Sonoran Desert and evergreen oak woodlands of AZ and NM
296 (cluster groups 4 and 5, respectively, Fig. 3a, 4a, b, Tables 1, 2). The west-east climatic
297 contrast on Axis 1 can be seen on the W GAMS and Tmin maps and the north-south contrast
298 on Axis 2 on the Tmin map only (Fig. 3b, c). The contrast between the oceanic vegetation of
299 the Pacific Coast Ranges and the continental vegetation of the Rocky Mountains and
300 Intermountain Region was distinct, with few species in common between the two zones or in
301 intermediate positions on the gradient (see Appendix S2 in supporting information, and the
302 low number of communities occurring at intermediate position along Axis 1 in Fig. 4b, i.e.,
303 only 12, 16, 8). Species occurring along the whole gradient of continentality were represented
304 by different subspecies in each zone, e.g., *Pinus ponderosa* var. *ponderosa*, *Pseudotsuga*
305 *menziesii* var. *menziesii* and *Pinus contorta* var. *muryana* in the west vs. *P. ponderosa* var.
306 *scopulorum*, *P. menziesii* var. *glauca* and *P. contorta* var. *latifolia* in the east.

307 RDA Axis 3 was strongly correlated with summer water balance (S ARID; $r = -0.86$,
308 Appendix S3, Fig. 4c) and also weakly with Tmin and GSL (Table 1). Within oceanic
309 climates, i.e., on the left of Axis 1, Axis 3 separated Mediterranean communities with a dry
310 summer (cluster 11 and 8 - CA evergreen oak forests and southern chaparral, respectively)
311 from temperate communities with a wet summer (clusters 1 and 12 - coastal temperate rain
312 forests and north-western subalpine forests, respectively). Within continental climates, i.e., on

313 the right of Axis 1, Axis 3 separated communities of the Great Basin with a dry summer, the
314 mountain Ponderosa pine woodlands and the piñon-juniper woodlands (clusters 2 and 3,
315 respectively), from mountain and subalpine coniferous forest communities of the Rocky
316 Mountains (cluster groups 9 and 7, respectively) with wet summers (Fig. 3a, 4d, Tables 2,
317 S1.1).

318 Oceanic climates with low W GAMS values always had high Tmin, but continental
319 climates with high W GAMS values were highly variable in Tmin (Fig. 5a), consistent with
320 the high positive correlation with RDA Axis 1 (Table 1, Fig. 3b, c). In contrast, there was no
321 correlation between W GAMS and S ARID (Fig. 5b), which is consistent with the co-linearity
322 with the two different RDA Axes, 1 and 3, respectively (Table 1, Fig. 4). MAP and MAT
323 were only correlated with Axes 1 and 2 ($r = -0.80$ for the former and $r = -0.89$ for the latter),
324 Consistent to our second hypothesis, the Gams-angle index provided a better metric than
325 AETy and DEFy. AETy was correlated with both Axes 1 and 3 but with lower correlations
326 coefficients than W GAMS and S ARID ($r = -0.54$ and -0.54 , respectively, Fig. 4a and c).
327 DEFy was primarily correlated with Axis 2 ($r = -0.76$) and less with Axis 3 ($r = 0.38$; Table 1,
328 Fig. 4a and c), as shown by the two climagrams of Fig. 6 where aridity zones delimited using
329 DEFy were highly correlated with the vertical axis (growing season length, i.e., RDA axis 2),
330 both in the dry- and wet-summer climagrams (Fig. 6a and b, respectively). Thus, the two
331 three-dimension climagrams proposed here for western USA are conceptually very similar to
332 the climagram proposed by Michalet (1991) for Morocco, with rainfall continentality
333 distributed horizontally on the climagram, growing season length distributed vertically, and
334 water balance distributed obliquely on the climagram.

335 Discussion

336 We found that rainfall continentality and summer water balance captured two different facets
337 of plant stress. In agreement with our first hypothesis, across the entire breadth of climate we
338 measured, rainfall continentality corresponded much better with vegetation distribution, and
339 took priority over the length of the growing season and summer water balance. These results
340 are of paramount importance, both for our understanding of the relationship between drought-
341 related climate variables and plant physiology, and for predicting the ecological and
342 evolutionary responses of plant species to changing climate.

343 *Rainfall continentality and low water balance in the growing season, two different stresses for*
344 *plants*

345 The rainfall continentality Gams index adjusted for winter precipitation (Pache et al., 1996a)
346 was highly predictive of vegetation types – strongly separating those in the Pacific Coast
347 Range, from woodlands and desert communities in the Intermountain Region and Rocky
348 Mountains (see Daubenmire, 1946; Franklin & Dyrness, 1973; Waring & Franklin, 1979).
349 These vegetation types are the foundation for classification in the western USA (Brown et al.,
350 1998). This dramatic rainfall continentality gradient is induced by both a steep orographic
351 effect on the windward sides of the coastal ranges and a strong rain shadow effect occurring on
352 their leeward sides (Bach et al., 2013). Crucially, this continental/rain shadow-driven contrast
353 is independent of the summer water balance contrast of the northwest temperate climate (wet
354 summer) of western WA and OR to the south-western Mediterranean climate of CA (dry
355 summer) and the south-east subtropical climate of AZ and NM (wet summer) to the desert
356 Mediterranean climate (dry summer) of the Mojave Desert in eastern CA and Great Basin in
357 NE and eastern OR.

358 As noted, most correlations of vegetation distribution with climate in the western USA
359 have used growing season or annual water balance indices such as AET_y and DEF_y
360 (Stephenson, 1990; 1998). However, consistent to our second hypothesis these two metrics,
361 commonly used in biogeography to quantify drought stress, had a lower and more complex
362 explanative power than W GAMS. We found that AET_y was correlated with both Axes 1 and
363 3, and DEF_y to Axis 2. This may be due to the sensitivity of AET_y to winter and spring
364 precipitation and to summer precipitation, with the former increasing AET_y in oceanic
365 climates and the latter decreasing AET_y in Mediterranean climates (see Fig. 1). This explains
366 why annual AET_y does not capture key climate patterns (i.e., rainfall continentality and
367 summer water balance) and the vegetation differences associated with it. The high correlation
368 between DEF_y and Axis 2 is due to the increase in precipitation and decrease in temperature
369 with increasing altitude in mountain ranges, both contributing to decreasing DEF_y, as also
370 observed in the ombrothermal method (Bagnouls & Gaussen, 1953; Walter & Lieth, 1960).
371 This latter result is also consistent with changes in aridity zones of Emberger (1930) and
372 DEF_y with increasing altitude in the climagram of Michalet (1991) for Morocco and the two
373 climagrams for Western USA (Fig. 6), respectively. However, altitude has very large effects
374 on temperature (Rolland, 2003). Thus, this is not easy to disentangle the effects on vegetation
375 of DEF_y and length of the growing season (Ozenda, 1985; Grace, 1987).

376 T_{min} was also strongly correlated with RDA Axis 1, which is consistent with the tight
377 physical relationships between rainfall continentality, cloudiness, VPD and irradiance.

378 Correspondingly, oceanic climates have high winter precipitation and high night temperatures
379 in the winter (Waring & Franklin, 1979; Bach et al., 2013). High VPD and irradiance
380 associated with rainfall continentality have strong effects on canopy microclimate and leaf
381 physiology (Michalet et al., 2003; Simonin et al., 2009; Novick et al., 2016). This facet of
382 drought is not captured in the indices of soil water deficit during the growing season
383 (Bagnouls & Gaussen, 1953; Stephenson, 1990). The winter Gams-angle index is a highly
384 effective way to capture this VPD-related component of drought.

385 Pache et al. (1996a) found that the geographical distribution of *Abies alba* in the
386 European Alps was highly correlated with the W GAMS index, with no occurrence of this
387 species in the most continental inner Central Alps. This is also the case for many *Abies*
388 species in the Mediterranean Basin, which only occur in the hyper humid Mediterranean
389 bioclimate characterized by high winter precipitation (Quezel & Médail, 2003 and see Fig. 2).
390 The common occurrence of North-American *Abies* species in the oceanic cluster groups in our
391 study is consistent with results from Europe and the Mediterranean Basin. Interestingly, the
392 two larch species in the study area, *Larix occidentalis* and *L. lyalii*, only occur in sites of
393 intermediate continentality (cluster groups 12 and 16), whereas in Europe *Larix decidua* is
394 common in the most continental inner zone of the European Alps. This may be due to the
395 higher rainfall continentality in the Rocky Mountains (W GAMS is always lower than 70° in
396 the Alps, vs. often over 85° in the Rocky Mountains; Pache et al., 1996a; see Fig. S3.3a in
397 Appendix S3).

398 Another ecological pattern that distinguishes rainfall continentality from summer
399 water balance is the relationship between the climatic distribution of tree species and their
400 responses to neighbours when seedlings. In the European Alps, Saccone et al. (2009) reported
401 that *A. alba* tolerated low summer water balance but not high air atmospheric stress (high
402 VPD) due to rainfall continentality. In this context, *A. alba* was facilitated by adult canopies
403 during the August 2003 European heat-wave. In contrast, *Picea abies* tolerated high
404 irradiance due to continentality, but was intolerant to low summer water balance. In turn, this
405 species was negatively affected by competition for water during the heat-wave. Similar results
406 were found by Muhamed et al. (2013) and Guignabert et al. (2020) for *Q. suber* and *Pinus*
407 *pinaster*, respectively, two Mediterranean species known for their oceanic distribution. In
408 their experiments, seedlings of both species were facilitated by the shade of shrubs in gaps
409 and forest dune communities from south-west France, correlated with lower VPD below
410 shrubs despite lower soil water availability than where shrubs were experimentally removed.

411 *Relative importance of rainfall continentality and water balance in western USA*

412 In the western USA, W GAMS values can be lower than 10° along the Pacific coast and
413 exceed 85° in the eastern Rocky Mountains, whereas in the European Alps the lowest values
414 are around 20° in the north-west and the highest values below 70° in the inner Central Alps
415 (Pache et al., 1996a; Michalet, 2001). The very high level of rainfall continentality observed
416 in California and Oregon, immediately to the east of the Sierra Nevada and Cascade Ranges,
417 only 300 km from the Pacific Coast, has its only parallel in Europe at a distance of at least
418 3000 km from the Atlantic Ocean, in the Ukraine. In contrast, except in western Washington,
419 summer water balance is very low in the western USA and thus varies much less spatially
420 than in Europe. This may explain the much higher relative importance of rainfall
421 continentality than summer water balance for vegetation distribution in western USA than in
422 Europe (Bagnouls & Gaussen, 1953). Additionally, the strong contrast existing along the
423 Pacific coast between the high winter rainfall and low summer rainfall (see Fig. 3 b and d),
424 and not in Europe along the Atlantic Ocean, may explain the rarity of deciduous tree species
425 in western north-America as compared to Europe and eastern north-America (Waring &
426 Franklin, 1979). One of the two deciduous oaks of the Rocky mountains, *Quercus gambelii*,
427 has been shown to occur in the southern Rockies but not the northern ones, because of the
428 higher summer rainfall of the latter due to the the American monsoon originating from the
429 gulf of Mexico (Neilson & Wullstein, 1983).

430 *Disentangling rainfall continentality from summer water balance for predicting responses to*
431 *climate change*

432 Disentangling rainfall continentality from low summer water balance is crucial for improving
433 the accuracy of our predictions for the effects of climate change on species distributions. Our
434 results indicate that many plant species, and in particular deep rooted woody species, in the
435 western USA may respond differently to changes in winter vs. summer precipitation. Neilson
436 (1986, 1987) have shown that past low-frequency variations in winter and summer rainfall
437 and temperatures drove the spatial dynamic of C3 and C4 species in the Chihuahuan Desert.
438 Our results also showed the ability of rainfall continentality to be strongly associated with
439 subspecies formation, with the three most common conifer species of western USA (*Pinus*
440 *ponderosa*, *Pinus contorta* and *Pseudotsuga menziesii*) represented by different subtaxons in
441 oceanic and continental climates along RDA Axis 1. This supports Ikeda et al. (2017) who
442 found that including genetically informed ecological niche models improved the accuracy of
443 predictions of species distributions under climate change. Thus, if the future climate becomes

444 drier in summer and thus more Mediterranean, or drier in winter and thus more continental,
445 we might predict strikingly different responses among woody plant species and their
446 subspecies. Most climate change studies have focused on summer, or growing season drought
447 stress (Breda, Huc, Granier, & Dreyer, 2006; Rehfeldt et al., 2006; Williams et al., 2020),
448 even though recent studies also indicate a trend towards increasing winter precipitation, as in
449 Scotland (UK) (Malby, Whyatt, Timmis, Wilby, & Orr, 2007) and in western US deserts
450 (Munson et al., 2013; Palmquist et al., 2016). Munson et al. (2013) have suggested that
451 increasing winter precipitation in western deserts should favour shrubs over grasses,
452 considering the current relative dominance of the former functional group in western deserts
453 characterized by higher winter than summer precipitation (Paruelo & Lauenroth, 1996; but see
454 Grover & Musick, 1990). In contrast, Palmquist et al. (2016) constructed models suggesting
455 that the benefits of higher winter rainfall for shrubs induced by climate change should be
456 overwhelmed by higher evaporative demand later in the growing season. Novick et al. (2016)
457 estimated that soil moisture supply and atmospheric demand for water independently limit
458 vegetation productivity and water use during periods of drought stress. The results of our
459 study support their conclusion - conceptual and mathematical models that do not
460 independently resolve VPD and soil moisture limitations (and thus rainfall continentality and
461 low water balance) will not adequately capture the magnitude of ecosystem response to
462 increasing climate stress. In conclusion, we argue that the Gams-angle index proposed here to
463 disentangle water balance from rainfall continentality has exceptional potential for predicting
464 species responses to climate change, as well as contribute to fundamental plant biogeography
465 (Bell, Bradford, & Lauentoth, 2014; Violle, Reich, Pacala, Enquist, & Kattge, 2014; Stevens,
466 Kling, Schwilk, Varner, & Kane, 2020).

467

468 References

- 469 Bach, A. J., Price, L. W., Dorn, R., Liu, T., & Phillips, F. (2013). *Mountain Climate,*
470 *Mountain Geography: Physical and Human Dimensions.* University of California Press,
471 Berkeley.
- 472 Bagnouls, F., & Gaussen, H. (1953). Saison sèche et indice xérothermique. *Bulletin de la*
473 *Société d'Histoire Naturelles de Toulouse*, 88, 193-239.

- 474 Barbour, M., Loidi, J., Garcia-Baquero, G., Meyer, R., & Whitworth V. (2014). The
475 composition and physiognomy of forest types are strongly linked to distance inland along
476 the northern California coast. *Phytocoenologia*, 44, 165-173. 10.1127/0340-
477 269X/2014/0044-0582
- 478 Bell, D. M., Bradford, J. B., & Lauenroth, W. K. (2014). Early indicators of change: divergent
479 climate envelopes between tree life stages imply range shifts in the western United States.
480 *Global Ecology and Biogeography*, 23, 168–180. 10.1111/geb.12109
- 481 Breda, N., Huc, R., Granier, A., & Dreyer, E. (2006). Temperate forest trees and stands under
482 severe drought: a review of ecophysiological responses, adaptation processes and long-
483 term consequences. *Annals of Forest Sciences*, 63, 625-644. 10.1051/forest:2006042
- 484 Brown, D. E., Reichenbacher, F., & Franson, S. E. (1998). *Classification of North American*
485 *biotic communities*. University of Utah Press, Salt Lake City.
- 486 Browning, K. A., & Hill, F. F. (1981). Orographic rain. *Weather*, 36, 326-329.
- 487 Caccianiga, M., Andreis, C., Armiraglio, S., Leonelli, G., Pelfini, M., & Sala, D. (2008).
488 Climate continentality and treeline species distribution in the Alps. *Plant Biosystems*, 142,
489 66-78. 10.1080/11263500701872416
- 490 Daubenmire, R. F. (1946). The life zone problem in the north intermountain region.
491 *Northwest Science*, 20, 28 38.
- 492 del Moral, R., & Watson, A. F. (1978). Gradient structure of forest vegetation in the central
493 Washington Cascades. *Vegetatio*, 38, 29–48.
- 494 De Martonne, E. (1926). Aréisme et Indice d'aridité. *Comptes Rendus Hebdomadaires des*
495 *Séances de l'Académie des Sciences*, Paris, 182, 1395-1398.
- 496 Desplanque, C., Rolland, C., & Michalet, R. (1998). Dendroécologie comparée du sapin et de
497 l'épicéa dans une vallée alpine française. *Canadian Journal of Forest Research*, 28, 737-
498 748. 10.1139/cjfr-28-5-737
- 499 Dray, S., & Dufour, A. B. (2007). The ade4 package: Implementing the duality diagram for
500 ecologists. *Journal of Statistical Software*, 22, 1-20. 10.18637/jss.v022.i04
- 501 Dray, S., Chessel, D., & Thioulouse, J. (2003). Co-inertia analysis and the linking of
502 ecological data tables. *Ecology*, 84, 3078-3089. 10.1890/03-0178

503 Emberger L., (1930). La végétation de la région méditerranéenne, essai d'une classification
504 des groupements végétaux. *Revue Générale de Botanique*, 42, 641-662 et 705-721.

505 Fick, S. E., & Hijmans, R. J. (2017). WorldClim 2: new 1-km spatial resolution climate
506 surfaces for global land areas. *International Journal of Climatology*, 37, 4302-4315.
507 doi:10.1002/joc.5086.

508 Frank, D. A., & Inouye, R. S. (1994). Temporal variation in actual evapotranspiration of
509 terrestrial ecosystems: patterns and ecological implications. *Journal of Biogeography*, 21,
510 401–411. 10.2307/2845758

511 Franklin, J. F., & Dyrness, C. T. (1973). Natural vegetation of Oregon and Washington.
512 USDA Forest Service Gen. Tech. Pacific Northwest Forest and Range Exper. Sta.,
513 Portland OR, Report PNW 8: 1417.

514 Gams, H. (1932). Die Klimatische Begrebzung von Pflanzenarealen und die Verteilung der
515 hygrischen Kontinentalität in den Alpen. *Zeitschrift der Geselchafften für Erkunde*, 56-68,
516 178-198.

517 Grace, J. (1987). Climatic tolerance and the distribution of plants. *New Phytologist*, 106, 113-
518 130.

519 Grover, H. D., and Musick, B. (1990). Shrubland encroachment in southern New Mexico,
520 U.S.A.: an analysis of desertification processes in the American Southwest. *Climatic*
521 *Change*, 17, 305-330. 10.1007/BF00138373

522 Guignabert, A., Augusto, L., Gonzalez, M., Chipeaux, C., & Delerue, F. (2020). Complex
523 biotic interactions mediated by shrubs: revisiting the stress-gradient hypothesis and
524 consequences for species survival. *Journal of Applied Ecology*, doi: 10.1111/1365-
525 2664.13641

526 He, W., Zhang, B., Zhao, F., Zhang, S., Qi, W., Wang, J., & Zhang, W. (2016). The Mass
527 Elevation Effect of the Central Andes and Its Implications for the Southern Hemisphere's
528 Highest Treeline. *Mountain Research Development*, 36, 213-221. 10.1659/MRD-
529 JOURNAL-D-15-00027

530 Ikeda, D. H., Max, T. L., Allan, G. J., Lau, M. K., Shuster, S. M., & Whitham, T. G. (2017).
531 Genetically informed ecological niche models improve climate change predictions. *Global*
532 *Change Biology*, 23, 164–176. 10.1111/gcb.13470

- 533 Jaccard, P. (1901). Etude de la distribution florale dans une portion des Alpes et du Jura.
534 *Bulletin de la Société Vaudoise des Sciences Naturelles*, 37, 547-579.
- 535 Kaufman, L. & Rousseeuw, P. J. (2009). *Finding groups in data: an introduction to cluster*
536 *analysis*. Vol. 344. John Wiley & Sons.
- 537 Maechler, M., Rousseeuw, P., Struyf, A., Hubert, M., & Hornik, K. (2019). Cluster: Cluster
538 Analysis Basics and Extensions. R package version 2.0.8.
- 539 Malby, A. R., Whyatt, J. A., Timmis, R. J., Wilby, R. L., & Orr, H. G. (2007). Long-term
540 variations in orographic rainfall: analysis and implications for upland catchments.
541 *Hydrological Sciences Journal*, 52, 276-291. 10.1623/hysj.52.2.276
- 542 Manuel, N., Cornic, G., Aubert, S., Choler, P., Bligny, R., & Heber, U. (1999). Protection
543 against photoinhibition in the alpine plant *Geum montanum*. *Oecologia*, 119, 149-158.
544 10.1007/s004420050771
- 545 Michalet, R. (1991). Nouvelle synthèse bioclimatique des milieux méditerranéens.
546 Application au Maroc septentrional. *Revue d'Ecologie Alpine*, 1, 45-60.
- 547 Michalet, R., Rolland, C., Joud, D., Gafta, D., & Callaway, R. M. (2003). Associations
548 between canopy and understory species increase along a rainshadow gradient in the Alps:
549 habitat heterogeneity or facilitation? *Plant Ecology*, 165, 140-160.
550 10.1023/A:1022297624381
- 551 Miller, D. A., & White, R. A. (1998). A Conterminous United States Multi-Layer Soil
552 Characteristics Data Set for Regional Climate and Hydrology Modeling. *Earth*
553 *Interactions*, 2. [Available on-line at <http://EarthInteractions.org>]
- 554 Muhamed, H., Le Bagousse-Pinguet, Y., Touzard, B., & Michalet, R. (2013). The role of
555 biotic interactions for the early establishment of oak seedlings in coastal dune forest
556 communities? *Forest Ecology & Management*, 297, 67-74. 10.1016/j.foreco.2013.02.023
- 557 Munson, S. M., Muldavin, E. H., Belnap, J., Peters, D. P. C., Anderson, J. P., Reiser, M. H.,
558 ... Christiansen, T. A. (2013). Regional signatures of plant response to drought and
559 elevated temperature across a desert ecosystem. *Ecology*, 94, 2030–2041. 10.1890/12-
560 1586.1
- 561 Neilson, R. P. (1986). High-Resolution Climatic Analysis and Southwest Biogeography.
562 *Science*, 232, 27-34. 10.1126/science.232.4746.27

563 Neilson, R. P. (1987). Biotic regionalization and climatic controls in western North America.
564 *Vegetatio*, 70, 135-147.

565 Neilson, R. P., & Wullstein, L. H. (1983). Biogeography of Two Southwest American Oaks in
566 Relation to Atmospheric Dynamics. *Journal of Biogeography*, 10, 275–297.
567 10.2307/2844738

568 Novick, K. A., Ficklin, D. L., Stoy, P. C., Williams, C. A., Bohrer, G., Oishi, A. C., ...
569 Phillips, R. P. (2016). The increasing importance of atmospheric demand for ecosystem
570 water and carbonfluxes. *Nature Climate Change*, 6, 1023-1027. 10.1038/NCLIMATE3114

571 Ozenda, P. (1985). *La végétation de la chaîne alpine dans l'espace montagnard européen*.
572 Masson, Paris.

573 Pache, G., Michalet, R., & Aimé, S. (1996a). A seasonal application of the Gams (1932)
574 method, modified Michalet (1991): The example of the distribution of some important
575 forest species in the Alpine chain. *Dissertation Botanicae*, 258, 31-54.

576 Pache, G., Aimé, S., & Michalet, R. (1996b). A simple model for the study of the altitudinal
577 rainfall gradient, applied in the Tyrolian orographic complex. *Revue d'Ecologie Alpine*, 3,
578 13-20.

579 Palmquist, K. A., Schlaepfer, D. R., Bradford, J. B., & Lauenroth, W. K. (2016). Mid-latitude
580 shrub steppe plant communities: climate change consequences for soil water resources.
581 *Ecology*, 97, 2342-2354. 10.1002/ecy.1457

582 Paruelo, J. M., & Lauenroth, W.K. (1996). Relative abundance of plant functional types in
583 grasslands and shrublands of North America. *Ecological Applications*, 6, 1212–1224.
584 10.2307/2269602

585 Peyre, C. (1983). Etagement de la végétation et gradients climatiques dans le système
586 atlasique marocain. Le bassin de l'Oued Rdat et le versant sud de l'Atlas au méridien du
587 Tizi N'Tichka. *Bullutein de la Faculté des Sciences, Sciences de la Vie, Marrakech*, 2, 87-
588 139.

589 Quézel, P., & Médail F. (2003). *Ecologie et biogéographie des forêts du bassin*
590 *méditerranéen*. Elsevier, Paris. R Core Team (2017).

591 R: A language and environment for statistical computing. R Foundation for Statistical
592 Computing, Vienna, Austria. URL <https://www.R-project.org/>.

593 Rehfeldt, G. E., Crookston, N. L., Warwell, M. V., & Evans, J. S. (2006). Empirical analyses
594 of plant-climate relationships for the western United States. *International Journal of Plant*
595 *Sciences*, 167, 1123-1150. 10.1086/507711

596 Reinhardt, K., McAbee, K., & Germino, M. J. (2019). Changes in structure and physiological
597 functioning due to experimentally enhanced precipitation seasonality in a widespread shrub
598 species. *Plant Ecology*, 220, 199-211. 10.1007/s11258-018-0845-z

599 Roe, G. H. (2005). Orographic precipitation. *Annual Review of Earth and Planetary Sciences*,
600 33, 645-671. 10.1146/annurev.earth.33.092203.122541

601 Rolland, C. (2003). Spatial and Seasonal Variations of Air Temperature Lapse Rates in
602 Alpine Regions. *Journal of Climate*, 16, 1032-1046. 10.1175/1520-
603 0442(2003)016<1032:SASVOA>2.0.CO;2

604 Rueda, M., Godoy, O., & Hawkins, B. A. (2018). Trait syndromes among North American
605 trees are evolutionarily conserved and show adaptive value over broad geographic scales.
606 *Ecography*, 41, 540–550. 10.1111/ecog.03008

607 Saccone, P., Pagès, J. P., Delzon, S., Brun, J. J., & Michalet, R. (2009). The role of biotic
608 interactions in altering tree seedling responses to an extreme climatic event. *Journal of*
609 *Vegetation Science*, 20, 403-414. 10.1111/j.1654-1103.2009.01012.x

610 Schermerhorn, V. P. (1967). Relations between topography and annual precipitation in
611 Western Oregon and Washington. *Water Resources Research*, 3, 707-711.
612 10.1029/WR003i003p00707

613 Simonin, K. A., Santiago, L. S., & Dawson, T. E. (2009). Fog interception by *Sequoia*
614 *sempervirens* (D. Don) crowns decouples physiology from soil water deficit. *Plant Cell*
615 *Environment*, 32, 882-892. 10.1111/j.1365-3040.2009.01967.x

616 Stephenson, N. L. (1990). Climatic Control of Vegetation Distribution - the Role of the
617 Water-Balance. *American Naturalist*, 135, 649-670. 10.1086/285067

618 Stephenson, N. L. (1998). Actual evapotranspiration and deficit: biologically meaningful
619 correlates of vegetation distribution across spatial scales. *Journal of Biogeography*, 25,
620 855-870. 10.1046/j.1365-2699.1998.00233.x

- 621 Stevens, J. T., Kling, M. M., Schwilk, D. W., Varner, J. M., & Kane, J. M. (2020).
622 Biogeography of fire regimes in western US conifer forests: A trait-based approach."
623 *Global Ecology and Biogeography*, 29, 944-955. 10.1111/geb.13079
- 624 Violle, C., Reich, P. B., Pacala, S. W., Enquist, B. J., & Kattge, J. (2014). The emergence and
625 promise of functional biogeography. *Proceedings of the National Academy of Sciences*
626 *USA*, 111, 13690–13696. 10.1073/pnas.1415442111
- 627 Walter, H., & Lieth, H. (1960). *Klimadiagramm Weltatlas*. G. Fischer, Jena.
- 628 Waring, R. H., & Franklin, J. F. (1979). Evergreen forests of the Pacific Northwest. *Science*,
629 4400, 1380-1386. 10.1126/science.204.4400.1380
- 630 Waring, R. H., Emmingham, W. H., Gholz, H. L., & Grier, C. C. (1978). Variation in
631 maximum leaf area of coniferous forests in Oregon and its ecological significance. *Forests*,
632 24, 131-140.
- 633 Williams, A. P., Cook, E. R., Smerdon, J. E., Cook, B. I., Abatzoglou, J. T., Bolles, K., ...
634 Livneh, B. (2020). Large contribution from anthropogenic warming to an emerging North
635 American megadrought. *Science*, 368, 314-318. 10.1126/science.aaz9600

636 Data accessibility statement

637 Data will available on Dryad (doi:10.5061/dryad.dbrv15f06)
638 <https://datadryad.org/stash/dataset/doi:10.5061/dryad.dbrv15f06>.

639

640 **Table 1:** Regression coefficients of the five variables of the RDA for the three axes and post-
 641 RDA correlations of the variables extracted from Worldclim with RDA scores. **: < 0.01,
 642 ***: < 0.001.

	RDA Axis 1	RDA Axis 2	RDA Axis 3
w.GAMS	0.99***	-0.06	0.05
w.PREC	-0.87***	0.12**	-0.01
Tmin	-0.63***	-0.72***	0.18***
GSL	-0.33***	-0.87***	0.14**
s.ARID	0.07	0.27***	-0.86***
<i>MAT</i>	-0.22***	-0.89***	0.22***
<i>MAP</i>	-0.80***	0.19***	-0.18***
<i>AETy</i>	-0.54***	0.30***	-0.54***
<i>DEFy</i>	0.30***	-0.76***	0.38***

643

644 **Table 2:** Vegetation labels, dominant species, continentality (position on RDA Axis 1, Fig.
 645 S3.3a), locations and vegetation zones (position on RDA Axis 2, Fig. S3.3b) of the 16 cluster
 646 groups. Vegetation zones correspond to GSL: high tropical: 10 months, low subtropical: 9 m.,
 647 high subtropical: 8 m., low temperate: 7 m., high temperate: 6 m., boreal: 5 m. Abbreviations:
 648 Rocky Mt. = Rocky Mountains, *Pseudotsuga menziesii m. or g.* = *Pseudotsuga menziesii var. menziesii* or
 649 *var. glauca*, *Pinus ponderosa p. or s.* = *Pinus ponderosa var. ponderosa* or *var. scopulorum*.

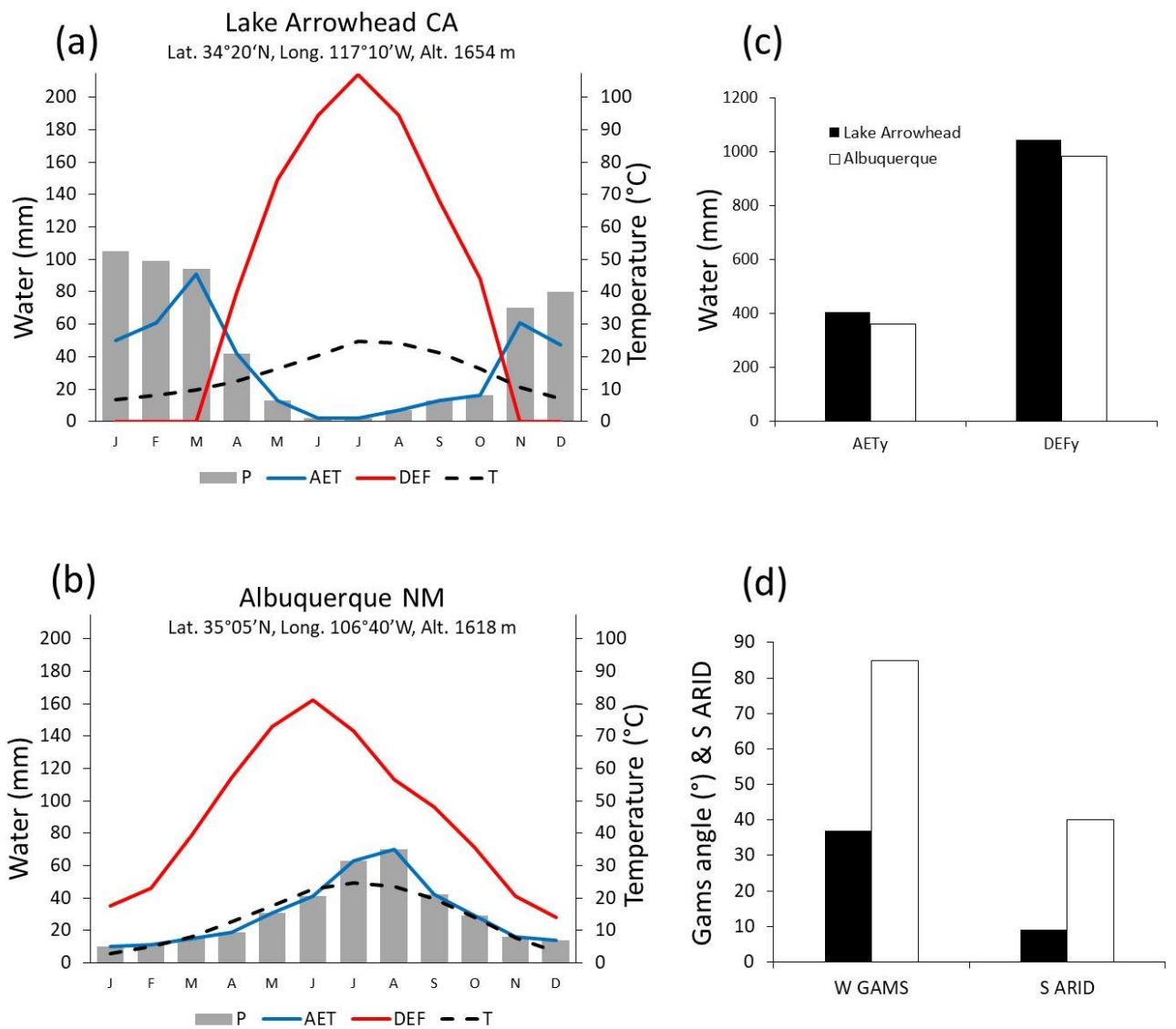
Cluster groups	Label Vegetation	Dominant Species	Continentality Location	Vegetation zone
11	Californian evergreen oak forests	<i>Quercus agrifolia</i> , <i>Q. douglasii</i> , <i>Q. wislizenii</i> , <i>Q. kelloggii</i> , <i>Q. chrysolepis</i>	Oceanic CA, OR	High subtropical and low temperate
1	Coastal rain temperate forests	<i>Pseudotsuga menziesii m.</i> , <i>Thuja plicata</i> , <i>Tsuga heterophylla</i>	Oceanic WA, OR, CA	Low and high temperate
8	Southern California Chaparral	<i>Quercus agrifolia</i> , <i>Q. douglasii</i> , <i>Ceanothus sp.</i> <i>Pseudotsuga macrocarpa</i>	Intermediate CA	Low and high subtropical
12	Northwestern Rocky Mt. subalpine forests	<i>Thuja plicata</i> , <i>Abies grandis</i> , <i>Pinus monticola</i> <i>Pseudotsuga menziesii g.</i> , <i>Larix occidentalis</i>	Intermediate ID, MT	High temperate and boreal
16	North western Rocky Mt. mountain forests	<i>Pseudotsuga menziesii g.</i> , <i>Larix occidentalis</i> , <i>Pinus ponderosa p.</i>	Intermediate MT, WA, ID	High temperate
4	Sonoran desert	<i>Cercidium microphyllum</i> , <i>Olneya tesota</i> , <i>Prosopis velutina</i> , <i>Opuntia sp.</i>	Continental AZ	High tropical and low subtropical
5	Eastern evergreen oak woodlands	<i>Quercus emoryi</i> , <i>Q. arizonica</i> , <i>Yucca sp.</i> , <i>Agave sp.</i>	Continental NM, AZ	Low and high subtropical
14	Mojave Desert	<i>Larrea tridentata</i> , <i>Ambrosia dumosa</i> , <i>Yucca brevifolia</i> , <i>Y. shedigera</i>	Continental CA, NM, UT	Low and high subtropical
10	Rocky Mt. pinion-juniper woodlands	<i>Pinus edulis</i> , <i>Juniperus osteosperma</i> , <i>Quercus gambelii</i> , <i>Artemisia tridentata</i>	Continental UT, NM, CO, AZ	High subtropical and low temperate

3	Great Basin pinion-juniper woodlands	<i>Pinus monophylla</i> , <i>Juniperus osteosperma</i> , <i>Artemisia tridentata</i>	Continental UT, NV, WY, CA	Low temperate
2	Great Basin mountain woodlands	<i>Pinus ponderosa</i> s., <i>Juniperus occidentalis</i> , <i>Artemisia tridentata</i> ,	Continental CA, OR, NM, ID	Low and high temperate
13	Northeastern mountain woodlands	<i>Pinus ponderosa</i> s., <i>Juniperus scopulorum</i> , <i>Artemisia frigida</i> , <i>A. cana</i>	Continental MT, WY	Low and high temperate
15	Great Basin sagebrush steppe	<i>Artemisia tridentata</i> , <i>Chrysothamnus nauseosus</i>	Continental ID, OR, WA	Low and high temperate
6	North eastern Rocky Mt. woodlands	<i>Pseutsuga menziesii</i> g., <i>P. flexilis</i> , <i>Artemisia tridentata</i> , <i>Juniperus scopulorum</i>	Continental MT, WY, CO, ID	Low and high temperate
7	Southern Rocky Mt. mountain forests	<i>Pinus ponderosa</i> s., <i>Pseudotsuga menziesii</i> g., <i>Picea pungens</i> , <i>Abies concolor</i>	Continental NM, CO, AZ	High temperate
9	Eastern Rocky Mt. subalpine forests	<i>Abies lasiocarpa</i> , <i>Picea engelmannii</i> , <i>Pseudotsuga menziesii</i> g., <i>Pinus contorta</i>	Continental MT, WY, CO	Boreal

650

651

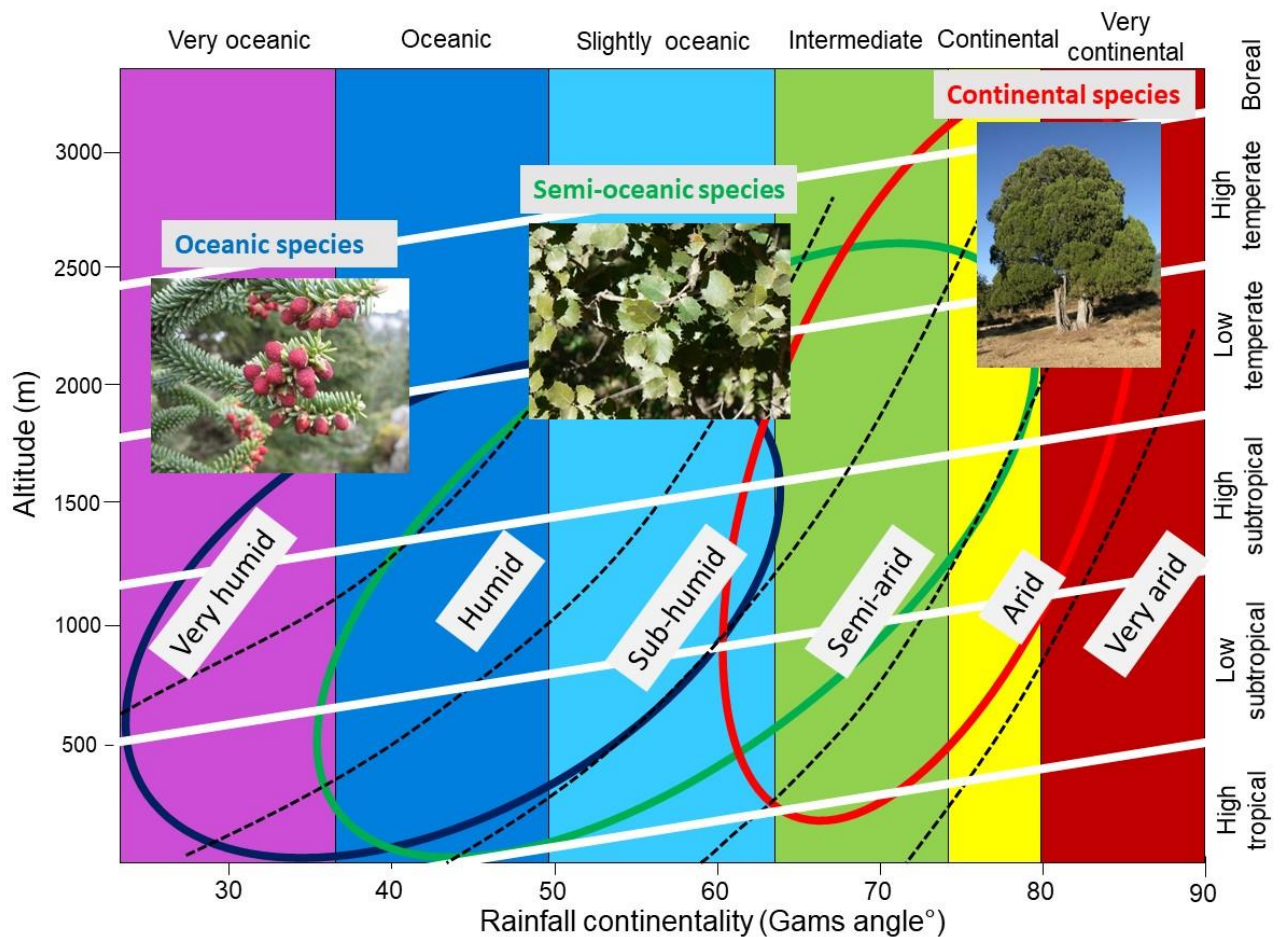
652 **Fig. 1:** Left: ombrothermal diagrams and actual evapotranspiration (AET) and deficit (DEF)
 653 of weather stations with oceanic Mediterranean (a) and continental subtropical (b) climates
 654 from similar latitude and altitude. Right panels show that annual AET (AETy) and DEF
 655 (DEFy) (c) are very similar, although rainfall continentality (W GAMS) and summer water
 656 balance (S ARID) (d) are very different. Note that the vegetation of stations (a) and (b) were
 657 classified in cluster 11 and 5 in Table 2, i.e., CA evergreen oaks and eastern evergreen oak
 658 woodlands, respectively.



659

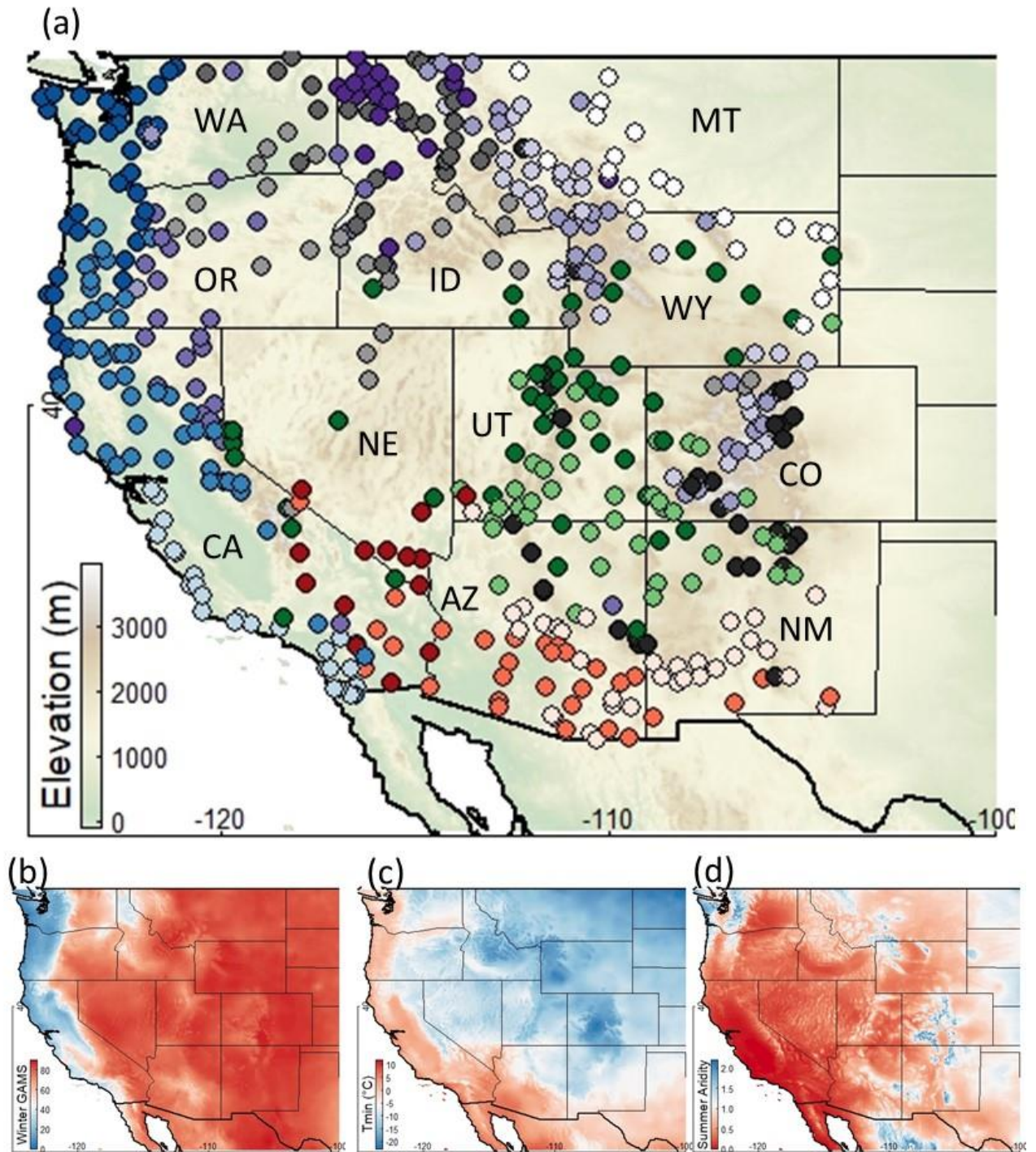
660

661 **Fig. 2:** Distribution of oceanic (in blue, from high to low altitude *Abies pinsapo* ssp.
662 *Moroccana* in the picture and *Quercus canariensis*, *Quercus suber* and *Quercus coccifera*),
663 semi-oceanic (in green, from high low altitude *Cedrus atlantica*, *Quercus rotundifolia* in the
664 picture and *Tetraclinis articulata*) and continental species (in red, from high to low altitude
665 *Juniperus thurifera* in the picture, *Juniperus phoenicea* and *Stipa tenacissima*) from Morocco
666 within the climagram of Michalet (1991). The climagram includes a horizontal axis for the
667 rainfall continentality gradient quantified with the annual Gams angle index (driving VPD and
668 cold stresses), a vertical axis for the altitudinal gradient (driving the length of the growing
669 season) and, in an oblique dimension, the water balance gradient calculated with the
670 Emberger index (1930). The latter was inspired by the De Martonne (1926) aridity index and
671 is primarily based on the ratio of annual precipitation to mean temperature. Coloured frames
672 along the horizontal axis represent the different zones of continentality delimited using the
673 annual Gams angle index and oblique plain white lines along the vertical axis delimit the
674 vegetation belts in relation to altitude and latitude (see also legend of Table 2 for GSL).
675 Oblique dashed lines delimit the aridity zones of Emberger (1930) indicated with white
676 frames.



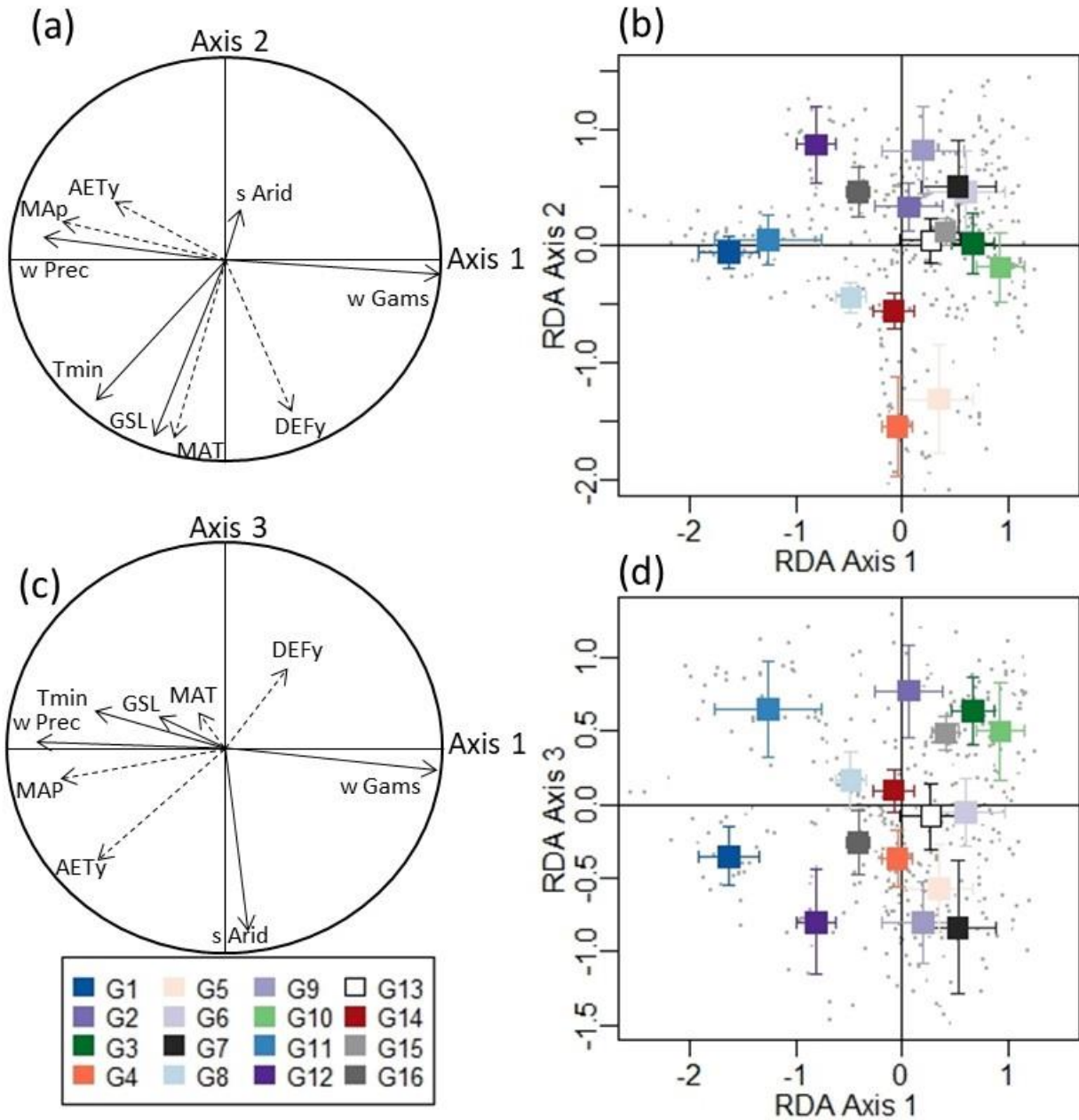
677

678 **Fig. 3:** Location of our 467 plots and 16 cluster groups in the 11 states of western USA (a),
 679 and maps of W GAMS index (b), Tmin (c) and Summer Aridity (d). Color legends of symbols
 680 of cluster groups are in Fig. 4. Abbreviations: AZ: Arizona, CA: California, CO: Colorado,
 681 ID: Idaho, MT: Montana, NE: Nevada, NM: New Mexico, OR: Oregon, UT: Utah, WA:
 682 Washington State, WY: Wyoming.



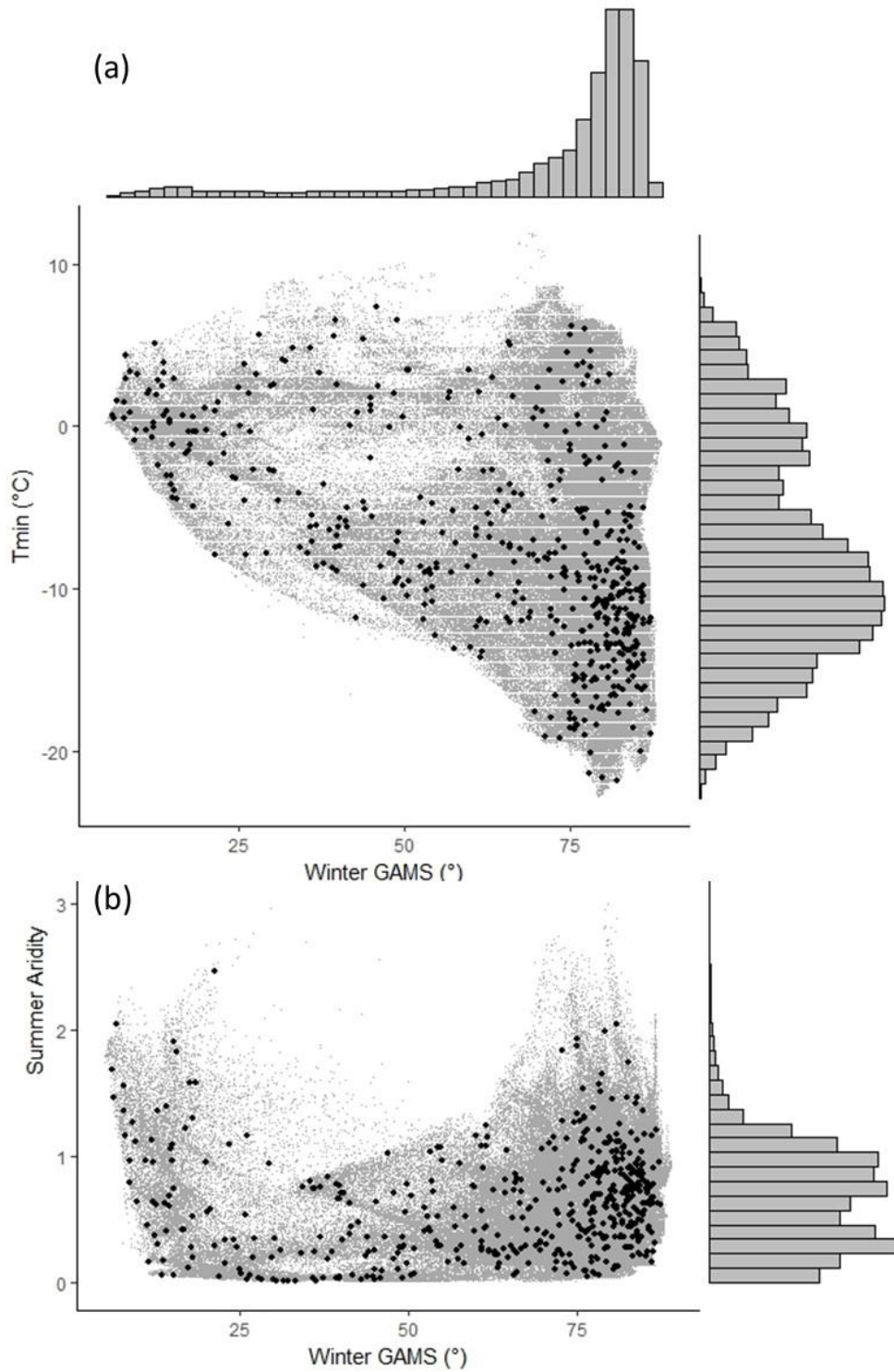
683

684 **Fig. 4:** RDA results, with in (a) 1-2 diagram for climate variables and in (b) for mean scores
 685 (± 1 SE) of the 16 cluster groups, and in (c) 1-3 diagram for climate variables and in (d)
 686 for mean scores (± 1 SE) of the 16 cluster groups. Dashed arrows in panels (a) and (c) show
 687 correlations for supplementary variables not included in the RDA.



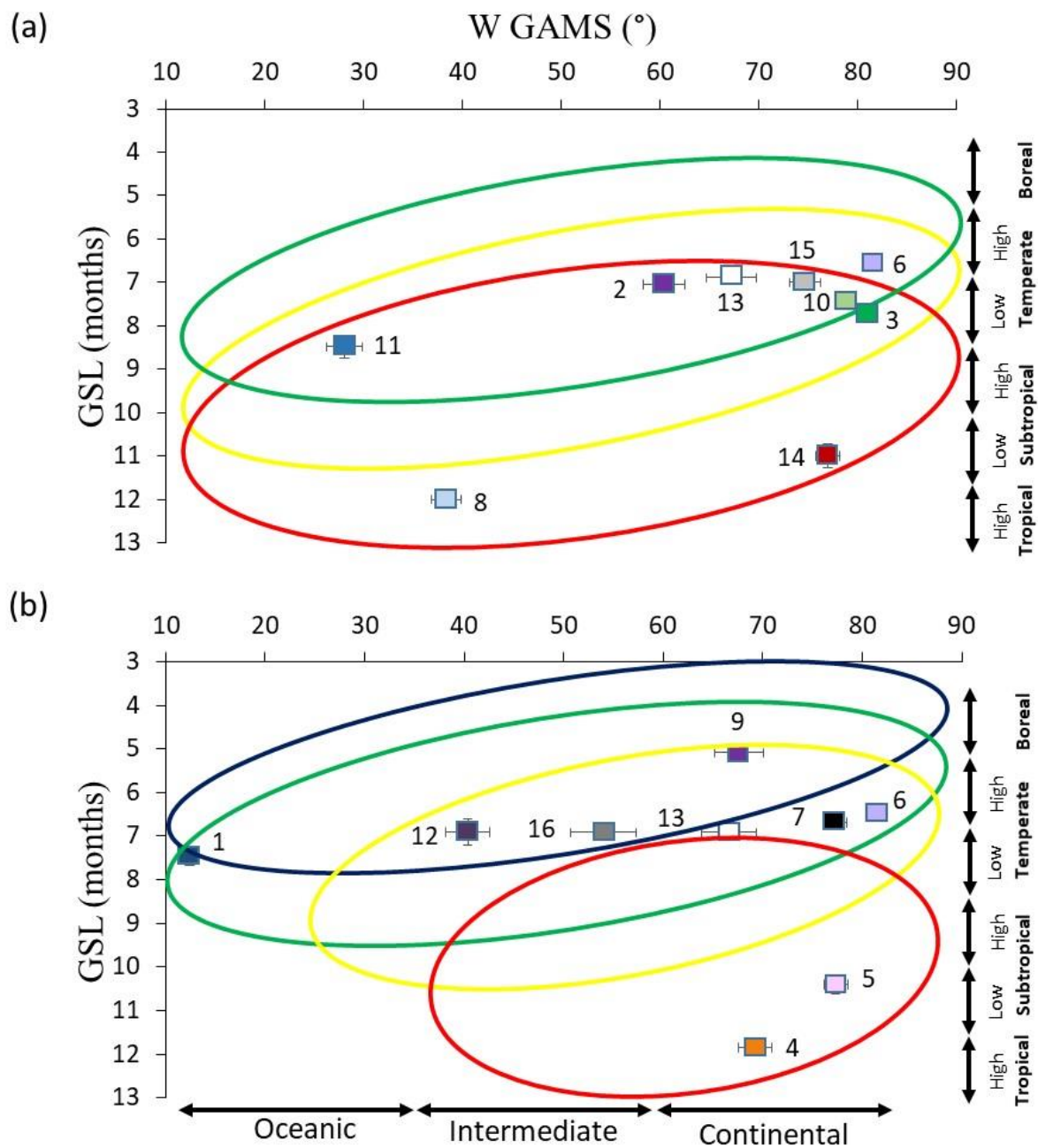
688

689 **Fig. 5:** Relationships between Tmin and W GAMS (a) and S ARID and W GAMS (b) for the
690 467 plots (black dots) and Worldclim datas (grey clouds).



691

692 **Fig. 6:** Mean (± 1 SE) positions of cluster groups from (a) dry-summer (upper part of RDA
693 axis 3, Fig. 3d) and (b) wet-summer sites (lower part of RDA axis 3, Fig. 3d) along the
694 rainfall continentality and growing-season length gradients. Ellipses delimit the positions of
695 sites with increasing DEFy following Stephenson (1998), with in blue humid (DEFy 38-200),
696 green sub-humid (DEFy 201-640), yellow semi-arid (DEFy 640-820) and red arid sites (DEFy
697 821-1770). Legends of cluster groups are indicated by their numbers and colours (see Fig. 4).
698 Continentality zones are indicated below the horizontal axis and vegetation belts along the
699 vertical axis (and see Table 2 for their delimitations).



700

701

702 **Short titles for the appendices:**

703 **Appendix 1:**

704 **Fig. S1.1:** Eigenvalues of the five RDA axes.

705 **Appendix 2:**

706 **Table S2.2:** Occurrence of species in the 16 cluster groups.

707 **Appendix 3:**

708 **Fig. S3.3:** Means (± 1 SE) of W GAMS (a), Tmin (b) and S ARID (c) for the 16 cluster
709 groups.

710